Environmental, exergetic and economic tradeoffs of catalytic- and fast pyrolysis-to-renewable diesel☆

S. Spatari [a, *, 1], V. Larnaudie [b], I. Mannoh [c], M.C. Wheeler [d], N.A. Macken [e], C.A. Mullen [f], A.A. Boateng [f]

[a] Civil, Architectural and Environmental Engineering, Drexel University, 3141 Chestnut St., Philadelphia, PA, 19104, USA
[b] Depto. Bioingeniería, Facultad de Ingeniería, Universidad de la República, Montevideo, CP 11300, Uruguay
[c] Department of Chemical and Biological Engineering, Drexel University, Philadelphia, PA, USA
[d] Chemical and Biomedical Engineering and Forest Bioproducts Research Institute, University of Maine, Orono, ME, 04469-5737, USA
[e] Department of Engineering, Swarthmore College, Swarthmore, PA, USA
[f] USDA-ARS, Eastern Regional Research Center, Wyndmoor, Pennsylvania, 19038, USA

ARTICLE INFO

ABSTRACT

This paper compares the cost and life cycle environmental performance of renewable diesel produced from upgraded catalytic fast pyrolysis (CFP) and fast pyrolysis (FP) bio-oils produced from forest residues. Integrating zeolite catalyst into the pyrolysis reactor in CFP requires upgrading in one catalytic hydro-cracking step, whereas FP requires upgrading by multiple catalytic hydrotreating and hydrocracking steps, raising capital costs. The FP system considers hydrogen production from co-produced biochar, further raising capital costs but eliminating the large external hydrogen need. Despite lower capital costs, due to higher operating costs from catalyst replacement and purchased hydrogen, the estimated mini-mum selling price of CFP fuel ($2/L) is greater than FP fuel ($1.68/L). Utilities, hydrogen and catalyst contributions to greenhouse gas (GHG) emissions, exergy and annual cost are sizeable for CFP. However, GHG emissions for CFP (-72 to 32 g CO_2e/MJ) are low and negative when considering credits for biochar due to a high biochar to fuel product ratio (2:1). In contrast, FP with catalytic upgrading maintains a high biofuel yield and low GHG emissions (8—13 g CO_2e/MJ) that meet energy policy objectives with more favorable economics compared to CFP. Neither fuel is cost competitive with petroleum-diesel even with renewable fuel credits.

© 2020 Elsevier Ltd. All rights reserved.

1. Introduction

Advanced biofuels are under development to meet policy objectives around the world to diversify energy supply and reduce greenhouse gas (GHG) emissions from the transportation sector. While research on biofuels has identified tradeoffs among environmental metrics related to biomass acquisition [1], they remain an important option for reducing the GHG intensity of liquid fuel markets if sourced from sustainably harvested biomass resources [2]. Thus, countries around the world have implemented renewable fuel policies [3–5] that aim to reduce GHG emissions from liquid fuel supply to short- and long-haul transportation markets, which incentivizes the production of transport fuels derived from biomass. Those policies rely on life cycle assessment (LCA) to judge a fuel's compliance in meeting greenhouse gas (GHG) reduction relative to baseline petrochemical fuels [6]. A biofuel's life cycle GHG emissions, described as its average fuel carbon intensity, influence its eligibility under key policies. For example, the federal Renewable Fuel Standard (RFS2) in the U.S [3] outlines a category defined as advanced fuels, where candidate biofuels must demonstrate a 50% reduction in life cycle GHG emissions relative to a baseline fuel, usually diesel or gasoline. European policy through the Renewable Energy Directive (RED) [5] and the U.K.'s Renewable Transport Fuel Obligation (RTFO) [4] also mandate reduction thresholds for biofuels relative to petroleum-based fuels.

The conversion of biomass to advanced transport fuels via biochemical and thermochemical conversion platforms aims to optimize biorefinery economics to produce fully oxygen-free (infrastructure compatible or "drop-in") fuels [7–11] and value added co-products [12], such as chemicals and polymers [13–16]. Within the thermochemical conversion platform is a set of pyrolysis and upgrading methods that hold much promise for reducing the GHG intensity of drop-in transport fuels, including aviation fuel [17] and renewable diesel and gasoline [18–23]. This paper focuses on two pathways for producing renewable diesel from forest residue feedstocks: catalytic fast pyrolysis (CFP) with hydrocracking and fast pyrolysis (FP) with catalytic upgrading via hydrotreating and hydrocracking, described as in-situ and ex-situ catalytic upgrading, respectively. Prior research on biomass fast pyrolysis and upgrading to value-added products has applied LCA to evaluate GHG emissions at small, e.g., up to 300 dry metric tons per day (MTPD) [17,23] and intermediate and large scales, e.g., 2000 MTPD [20]; multiple life cycle environmental impacts and economics related to biomass supply chains [24]; and the environmental benefits of biochar co-products [25], markets and policies [26]. Our goal is to evaluate the environmental and economic differences of in-situ and ex-situ catalytic upgrading of fast pyrolysis bio-oil to renewable diesel to meet U.S. RFS2 advanced fuel policy.

Upgrading fast pyrolysis bio-oil to oxygen-free fuels demands significant input of hydrogen [23,27] and catalysts [28] for hydrocracking and hydrotreating steps owing to the degradation of the catalysts and their need for regeneration in continuous production. Prior LCA research has developed life cycle inventories for catalysts used in fast pyrolysis upgrading [28,29]. These datasets, which track the complete cradle-to-gate manufacture of catalysts, are necessary inputs to understanding and optimizing process design of pyrolysis bio-oil upgrading systems where minimizing catalyst cost and environmental impact is a design variable. Snowden-Swan et al. [29] constructed life cycle inventories for NiMoS and Ru/C catalysts, the latter of which has a wide GHG intensity range per unit mass, which, at the upper bound combined with a short lifetime, compounds the net life cycle GHG emissions for biofuels produced from upgraded fast pyrolysis oil. Benavides et al. [28] showed that ZSM-5 and CoMo/γ-Al$_2$O$_3$ catalyst contributions to life cycle GHG emissions of renewable gasoline is significant on a life cycle basis, particularly if loading rates are high. The authors also studied the GHG emission of regeneration rates for platinum and molybdenum catalysts, which can be up to 11% and more than one third of the cradle-to-gate emissions for their manufacture, respectively. Our objective is to understand key differences among life cycle GHG emissions, cumulative exergy, as both an indicator of maximum theoretical work of the system and resource efficiency, and cost of in-situ and ex-situ catalytic upgrading of pyrolysis bio-oils, considering the effects of catalyst, hydrogen source and their loading.

2. Methods

2.1. System boundary

Life cycle assessment (LCA) and techno-economic analysis (TEA) are used to evaluate two fast pyrolysis and upgrading pathways (Fig. 1) to produce renewable diesel from forest residues in the U.S. Northeast in the state of Maine. Material and energy balances from experimental data are used to estimate the biorefinery scale-up cost and construct the life cycle inventory (LCI). The LCI models were developed from mass balances following ISO 14040/14044 standards [30,31]. One configuration employed catalytic fast pyrolysis (CFP) over a zeolite catalyst followed by hydrocracking over Ni/ZSM-5 with hydrogen produced from catalytic cracking of

naptha, in a one-step reactor with product yields based on experimental data by Mullen et al. [32], and for which the process simulation is described herein. The second configuration employed fast pyrolysis (FP) and catalytic upgrading in three sequential hydrotreating steps followed by hydrocracking all using a renewable source of hydrogen for hydrodeoxygenation based on a techno-economic analysis model by Carrasco et al. [33]. In both cases the excess co-produced biochar is assumed to either replace coal in power generation or be amended to land to replace soil organic carbon using assumptions from Pourhashem et al. [34]. We evaluate these alternative pathways using the life cycle impact assessment metrics, a) climate change, where GHG emissions are estimated using the 100-year global warming potential (GWP) equivalence factors measured in kg CO$_2$ equivalents (CO$_2$e), and b) cumulative exergy demand (CExD). Exergy (useful work) is a measure of the maximum theoretical work from a substance if it were in equilibrium with the environment. CExD [35], a measure of the total depletion of exergy associated with the conversion of material from its natural state to products, has been used as an indicator of resource use in renewable energy applications, including bioenergy [17,36]. We compare estimated production cost of each pathway using the minimum fuel selling price (MFSP) metric and compare differences among capital investment and operating costs. The functional unit defined is 1 MJ of renewable diesel that is produced and consumed for transportation in well-to-wheels (WTW) analysis. The renewable diesel pathways are compared to low S diesel fuel, which have a WTW GHG intensity of ~93 g CO$_2$e MJ^{-1} that have been applied in prior research [37]. Further details and supporting data are available in Appendix A.
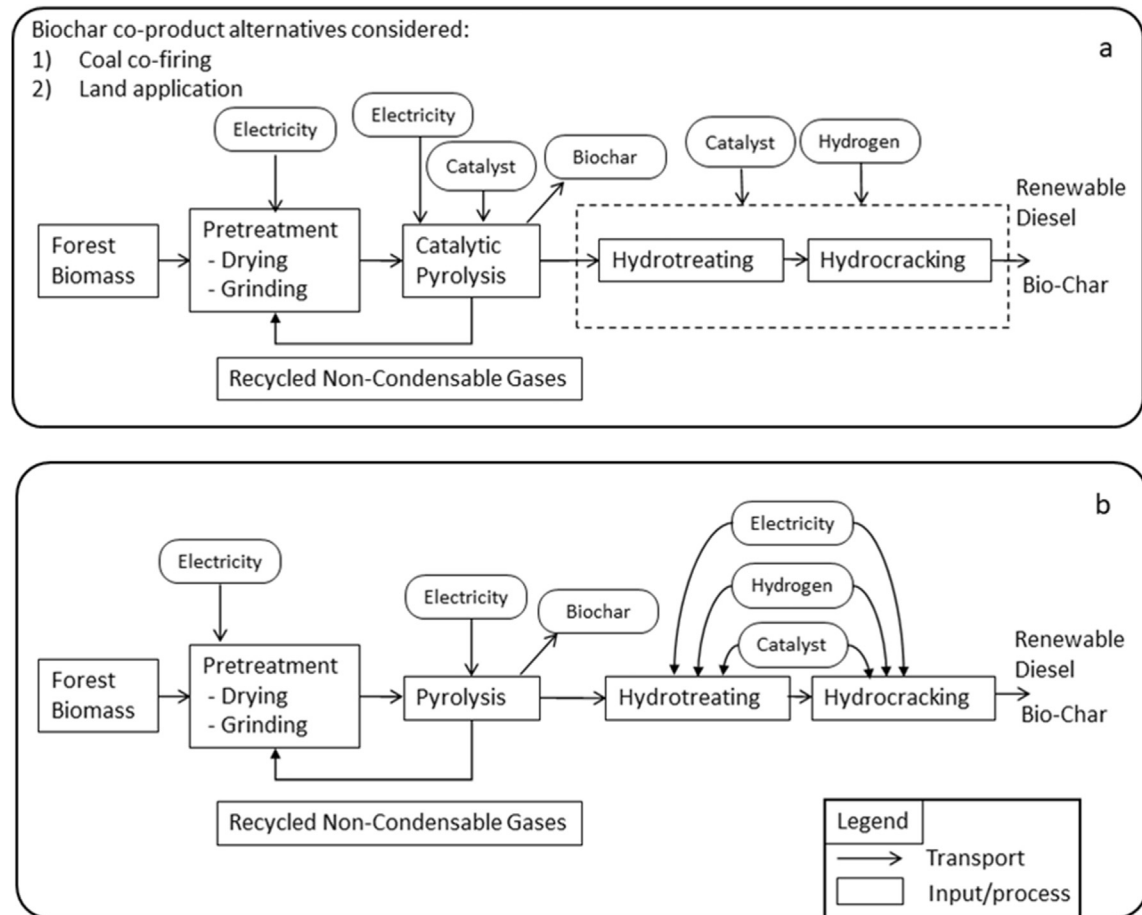
2.2. Life cycle inventory analysis

2.2.1. Biomass harvesting and transport

Supply of forest residues in the state of Maine, U.S.A., includes operations for harvesting, collecting, and transporting the feedstock using equipment operating on diesel fuel. Table 1 summarizes key input data on the basis of 1 kg of fast pyrolysis bio-oil used in the analysis along with exergy data from Keedy et al. [36]. The GHG emissions intensity of diesel fuel is assumed to be 93 g CO$_2$e/MJ [37] and its CExD is 43 MJ kg^{-1} [38].

2.2.2. Biomass conversion

Aspen Plus was used to size a 2000 dry metric ton per day (MTPD) catalytic fast pyrolysis (CFP) and upgrading biorefinery (Fig. 2), which was modified from a model of fast pyrolysis (FP) and catalytic upgrading developed by Carrasco et al. [33] to establish a material and energy balance for LCA and cost estimation for TEA modeling. Material balance data associated with each input and output flow in Fig. 2 are summarized in SI Tables S3 and S4. The CFP process design included heat integration for flue gas heat recovery as well as other units within the upgrading block. Also, energy was recovered by burning excess char and matching the heat with streams of suitable temperature differences and heat duties. Process flow diagrams for the CFP, upgrading, drying, and grinding sub-processes within the biorefinery are summarized in Figs. S1–S4 (Appendix A). Major differences between the processes include that the CFP process uses a catalyst in the fast pyrolysis reactor to reduce the oxygen content of the bio-oil; thus, it requires less hydrogen for deoxygenation through a hydrocracking process, and therefore uses purchased hydrogen for upgrading. The CFP process subjects forest residue biomass to catalytic pyrolysis over a zeolite catalyst to produce a bio-oil low in oxygen concentration, which then undergoes hydrodeoxygenation over Ni/ZSM-5 in one hydrocracking reactor. We compare the CFP process with fast pyrolysis (FP) and ex-situ catalytic upgrading according to the design

Fig. 1. System boundary for cradle-to-gate production of renewable diesel via a) catalytic pyrolysis over ZSM-5 and mild hydrotreating over Ru/C; and b) fast pyrolysis and catalytic upgrading.

Table 1
Life cycle inventory inputs for the production of 1 kg fast pyrolysis bio-oil from Keedy et al. [36].

Input Operations	Amount	Exergy	CExD
Feller buncher	0.00206 kg	0.089 MJ	0.117 MJ
Grapple-skidder	0.00344 kg	0.148 MJ	0.195 MJ
Chipper	0.00186 kg	0.08 MJ	0.105 MJ
Transportation	0.00496 kg	0.213 MJ	0.281 MJ
Total		0.53	0.698

specifications of Carrasco et al. [33]. Table 2 summarizes key design costs and differences among the two processes compared. Supporting information in Appendix A includes tables for size, scaling and installed cost of the CFP unit operations (Table S1) and assumptions applied in the cost analysis for the discount rate, interest rate, debt-equity ratio, inflation rate, capacity factor, and other factors (Table S2) that were taken from the design report of a 2000 MTPD biochemical conversion biorefinery by Humbird et al. [39],
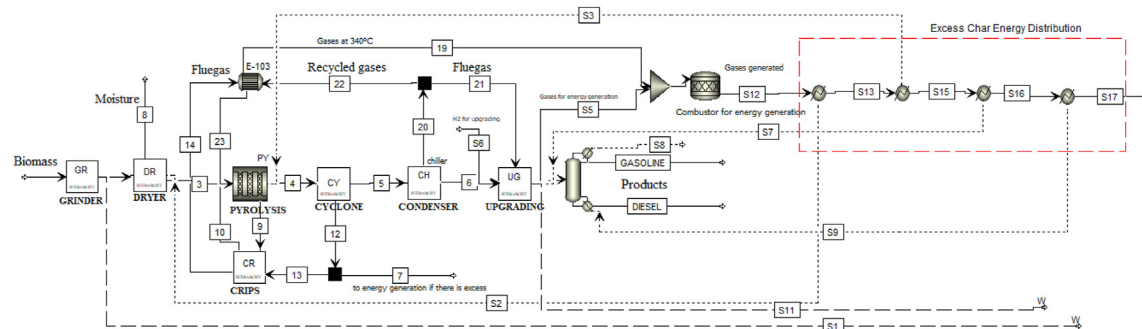
Fig. 2. Catalytic pyrolysis with hydrotreating of forest residues. The process described herein assumes production of renewable diesel as product and biochar as co-product. Red-dotted box shows area of energy recovery from excess char with heat exchangers that distribute energy to streams matched by temperature differences and heat duties.

Table 2
Select cost data for catalytic fast pyrolysis (CFP) with hydrocracking (upgrading) applied in this study and fast pyrolysis (FP) and catalytic upgrading from Carrasco et al. [33].

	Catalytic fast pyrolysis and upgrading 2015 USD	Fast pyrolysis and catalytic hydrotreating and hydrocracking 2015 USD[d]
Feedstock ($/dry metric ton)	69	69
Catalyst		
Pyrolysis:		
zeolite ($/kg)	22.6[a]	N/A
Upgrading:		
CoMo ($/kg)		30
Ni/ZSM-5 ($/kg)	10[a]	5
Ru/C ($/kg)	N/A	60
Hydrogen ($/kg)	4.82[b]	0
Utilities		
Cooling water ($/metric ton)	0.27[c]	0.27
Electricity ($/kWh)	0.06[c]	0.06
Ash disposal ($/metric ton)	53[c]	53
Wastewater treatment ($/m³)	0.34[c]	0.34

N/A is not applicable.
[a] Catalyst costs were taken from Dutta et al. [44] and were adjusted to 2013 U S. dollars using data extrapolated from SRI International Chemical Economics Handbook, Economic Environment of the Chemical Industry 2004.
[b] Hydrogen costs were taken from Dillich et al. [45] and were adjusted to 2013 U S. dollars using data extrapolated from SRI International Chemical Economics Handbook, Economic Environment of the Chemical Industry 2004.
[c] Utility costs for cooling water, electricity, ash disposal and wastewater treatment were taken from Turton et al. [46] and reflect 2015 U S. dollars.
[d] All costs for the fast pyrolysis and catalytic upgrading were taken from Carrasco et al. [33] and reflect 2015 U S. dollars.

Table 3
Material Inventory for catalytic fast pyrolysis (CFP) with one-step hydrocracking and fast pyrolysis (FP) with three stages of catalytic hydrotreating, followed by hydrocracking.

Biorefinery Input	CFP + hydrocracking	FP + catalytic hydrotreating and hydrocracking	Unit
Forest residue	1000	1000	metric tons
zeolite (catalytic pyrolysis)	2898		
Ni/ZSM-5 (hydrocracking)	336	123	kg
Ru/C		100	kg
Co/Mo		704	kg
Hydrogen	9777		kg
Cooling water	19,300	64,950	m³
Electricity	128,00	219,300	kWh
Ash	37	37	Metric tons
Renewable diesel	96,600	163,000	kg
Biochar (co-product)	195,000	16,000	kg

and used to estimate the minimum fuel selling price of the renewable diesel product. Both CFP and FP processes described herein were modeled based on experiments carried out in a bench scale pyrolysis unit at the U.S. Department of Agriculture's Agricultural Research Service laboratory. The pyrolysis unit experiments used woody biomass feedstocks, where the FP process used hog fuel, a secondary woody residue from mill residues, and the CFP experiments used white oak. The bio-oil compositions were different not only due to the presence of the catalyst in the reactor, but also due to biomass substrate. In both cases, the feedstock is modeled to be sourced from forest and mill residues, which are assumed to have minimum land use change impacts and changes to forest carbon stocks. However, significant changes to forest carbon

stocks can lead to high net GHG emissions depending on the scale of forest biomass use and time needed for forests to regenerate [40,41].

Material and energy inputs to the CFP and FP processes were derived from the Aspen Plus material balances (Table 3) and are the energy and material basis for the biomass conversion step in the life cycle inventory (LCI). The LCI model was built using SimaPro 8.4 with electricity supply from the NPCC electricity grid, assuming the biorefinery would be located in the state of Maine. Hydrogen is assumed to be supplied from petroleum refinery hydrocracking operations but could also be supplied from methane reforming. Data on catalysts were sourced from ecoinvent [42], GREET [28,43] and literature [29] and are discussed in Section 2.2.3. Ash disposal

Table 4
Daily catalyst and input quantity for FP and CFP processes.

	FP + Catalytic Upgrading		CFP + hydrocracking	
	Catalyst	Quantity (kg/day)	Catalyst	Quantity (kg/day)
Fast Pyrolysis Catalyst	N/A		zeolite	2898
Upgrading Catalyst	Ni/ZSM-5	123	Ni/ZSM-5	336
	Co/Mo	704		
	Ru/C	101		

Notes: N/A is not applicable.

and wastewater treatment steps are also assumed from unit processes from ecoinvent [42]. Both processes co-produce biochar, which we assume is either used as a co-feed with coal for power production or as a land amendment according to research by Pourhashem et al. [34].

2.2.3. Catalyst assumptions

Daily catalyst loadings are specified according to expected degradation discussed by Dutta et al. [44]. Life cycle inventory data for the replacement of zeolite, Ni/ZSM-5, Ru/C and Co/Mo are taken from the ecoinvent database [42] and from a study by Benavides et al. [28], based on catalyst specifications by Jones et al. [47], and applied the GREET catalyst module [43]. Table 4 summarizes daily catalyst replacement assumptions we apply, which are factored into the mass balance (Table 3) for baseline calculations. We examine the sensitivity of GHG emissions from the the biofuel pathways to changes in catalyst GHG intensity and loading based on literature studies (SI Table S6 summarizes boundary settings). For example, we use data from ecoinvent [42] to characterize the GHG emissions intensity of zeolite and ZSM-5 catalysts (5.1 kg CO_2e/kg) and compare results to those estimated by Benavides et al. [28] for ZSM-5 (7.7 kg CO_2e/kg). Moreover, we test the effect of a $\pm$ 25% loading of zeolite and ZSM-5 in both CFP and FP pathways suggested by the authors. For the FP system, in addition to testing variability in the ZSM-5 catalyst, we test the effect of changing the Ru/C lifetime to 30- and 330-days relative to the 60-day lifetime described by Carrasco et al. [33] and the effect of the Ru/C catalyst's GHG intensity based on a study by Snowden-Swan et al. [29], who estimated a range of 13.7–80.4 kg CO_2e/kg for the catalyst.

2.2.4. Hydrogen supply for bio-oil deoxygenation

Pyrolysis bio-oil upgrading demands a large input of hydrogen, which raises operating costs given the high market price of hydrogen ($4.82 kg^{-1}) used for hydrodeoxygenation to produce drop-in fuels [23]. One of the goals of catalytic pyrolysis is to reduce the oxygen content of the bio-oil, which also reduces hydrogen demand in process steps following the fast pyrolysis unit. For the two conversion processes we compare, the bio-oil from the CFP system has 17.9 wt % oxygen, whereas the bio-oil from fast pyrolysis has 39 wt % oxygen. Thus, the CFP process aims to minimize hydrogen costs by reducing the oxygen content in the bio-oil, thereby also reducing the capital costs of upgrading (see review by Sorunmu et al. [48]), where only one reactor for hydrocracking is needed to produce renewable diesel (Fig. 2). Whereas in the upgrading of FP bio-oil aims to reduce H_2 costs by producing them from co-produced biochar from FP. Carrasco et al. [33] specify producing hydrogen by first gasifying the co-produced biochar to generate syngas according to specifications by Worley and Yale [49]; second steam reforming of the syngas; and third employing water-gas shift reactors and purification to produce hydrogen. The hydrogen used is thus sourced from the biomass and reduces total input of fossil fuels from biorefinery and eliminates the need for external hydrogen supply.

3. Results and discussion

3.1. Techno-economic analysis

Capital and operating costs for the CFP process were calculated in 2015 U S. dollars and equipment was sized for operating at 2000 MTPD, the same basis used by Carrasco et al. [33] for FP, which we compare to CFP. Operating costs are divided among variable and operating costs (Table 5) and reflect the fact that annual catalyst replacement makes up 1.4% and 28% of annual costs for hydrocracking and CFP, respectively; and hydrogen costs make up 20% of

Table 5
Annual operating costs and estimated revenue of CFP with one-step hydrocracking and FP with three stages of catalytic hydrotreating, followed by hydrocracking.

Pathway:	CFP (million 2015$)	FP (million 2015$)
Capacity:	2000 MTPD	2000 MTPD[a]
Variable Costs:		
Raw materials	48.30	45.3
Catalyst:		
Catalytic pyrolysis (zeolite)	65.36	N/A
Hydrotreating (FP)/Hydrocracking (CFP&FP):		
Ru/C	N/A	4.23
Co/Mo	N/A	16.8
Ni/ZSM-5	3.36	0.43
Hydrogen	47.09	N/A
Cooling water	52.17	
Electricity	7.69	
Total utilities	59.86	25.5
Wastewater treatment	0.08	1.6
Waste treatment (ash)	1.66	1.66
Fixed Costs:		
Labor	2.90	1.64
Labor burden (90%)	2.61	
Maintenance and overhead	1.82	32.2
Property insurance	0.88	
Distribution and selling		7.48
Other costs		18.2
Total costs	**235.63**	**154**
MFSP ($/L)	2.00	1.68
Total Revenue from sales	**234**	**213**

Notes: N/A is not applicable.
[a] Operating cost data are described in Carrasco et al. (2017) [33]; total utilities cost include water, cooling water and electricity.

Table 6
Capital Costs of CFP with one-step hydrocracking and FP with three stages of catalytic hydrotreating, followed by hydrocracking[a].

	CFP (million 2015$)	FP (million 2015$)
	2000 MTPD[b]	2000 MTPD[c]
Equipment		
Pretreatment	10.5	13
Pyrolysis area	48.4	67
Gas combustion and separation	17.8	
Upgrading and separation	31.5	121
Energy generation		7.4
Hydrogen production		75
Storage	0.2	2.4
Total installed equipment	108.5	285.5
Warehouse, site development	17.1	
Total direct costs	125.6	
Total indirect costs	75.4	
Fixed capital investment (FCI)	201	
Land	1.8	
Working capital	10.1	
Total capital investment	212.9	427

[a] Major differences between the CFP and FP processes include that CFP consists of a one-stage hydrocracker, but the FP process includes three stages of hydrotreating (mild upgrading), separation, and a hydrocracking reactor.
[b] Total direct costs include 4%, 9%, and 4.5% of ISBL installed costs for warehouse, site developing and additional piping. Indirect costs are assumed to be 10% of total direct costs for prorateable expenses, field expenses, project contingency and other costs (start-up, permitting and others) and 20% for home office construction fees. The fixed capital investment includes a cost of $14,000/acre for land with 132 acres and working capital consisting of 5% of the fixed capital investment (FCI).
[c] Carrasco et al. [33] estimate the cost of a grassroots facility using the module costing technique, where contingency and fees represent 15% and 3% of the bare module cost an auxiliary fees are 50% of the base condition, consisting of the purchased cost of equipment.

operating costs, all significant portions of the total operating cost. Total revenue for the renewable diesel product is estimated from the minimum fuel selling price (MFSP) of renewable diesel required to achieve a zero net present value over the 30-year project life. Capital costs (Table 6) for CFP are lower than FP due to needing fewer unit operations for upgrading the bio-oil and using purchased hydrogen, thus having a lower total installed cost. The MFSP is high for both processes and on the upper end of projected estimates from TEA studies reviewed recently by Sorunmu et al. [48], which reported a range between $0.50 to $1.67 L^{-1}, the highest value being that of Carrasco et al. [33]. Although capital costs for CFP are about half of those for FP, its operating costs are higher. Hydrogen costs are a significant annual expense, in spite of a higher revenue stream. Table S1 in Appendix A lists individual costs, sizing factors, and data sources used for the CFP system.

3.1.1. Sensitivity of model parameters on minimum fuel selling price

We evaluated the sensitivity of specific cost parameters on the MFSP of renewable diesel produced from the CFP process. Upper and lower bounds for four cost parameters (catalyst cost, catalyst loading, feedstock cost and capital cost) and inclusion or exclusion of renewable fuel credits for which biofuels that fit the advanced biofuel category of RFS2 qualify. The renewable fuel credits were estimated based on the assumption of meeting the renewable identification number (RIN) D5 category for advanced biofuels (described in Section 3.2) and cellulosic waiver credits (CWC) based on average credit values over years 2013–2017 used by Brandt et al. [14] for aviation fuel, which meets the same D5 category and qualifies for CWC. Fig. 3, which examines the sensitivity of variable cost parameters, indicates that catalyst loading and upper bound cost can increase the MFSP most significantly, suggesting that reduction in loading and improvements in catalyst lifetime can both reduce the MFSP of renewable diesel via CFP to be more competitive with petroleum-based diesel. Moreover, variation in feedstock and capital cost can also raise or lower the MFSP. Renewable fuel credits (RIN and CWC) can significantly lower the MFSP, but would not make it competitive with low S diesel, whose average price is approximately $0.48 L^{-1}. While examining the sensitivity of multiple input parameters, Carrasco et al. [33], conclude that capital costs for the multiple hydrotreating and upgrading reactors, and on-site hydrogen generation are the most sensitive parameters affecting MFSP for FP.

3.2. Life cycle assessment

3.2.1. Life cycle GHG emissions

Fig. 4 shows the contribution of life cycle inputs, credits and the net life cycle GHG emissions, respectively, for the cradle-to-gate production of the two renewable diesel pathways. Two co-product credit scenarios taken from the work of Pourhashem et al. [34] were evaluated for the biochar co-product, for which the system boundary considers the cradle-to-grave fate of the biochar; one in which the biochar is used as a coal substitute in power generation and combusted to produce power, and the other in which the biochar is land-amended and remains part of soil organic carbon (SOC) stocks for more than the 100-year timeframe of the analysis. Fig. 4 shows the effects of changes in GHG emissions due to catalyst loading and catalyst GHG emissions intensity. In each case, system expansion was used to treat the effects of the biochar co-product, which displaces coal or is applied on agricultural land as an amendment. In all cases, the pathways would meet U.S Renewable Fuel (RFS2) guidelines for advanced fuels, with a more than 50% reduction in life cycle GHG emissions relative to a baseline fuel. Overall, the renewable diesel GHG emissions for each pathway falls within a close range of other pyrolysis-based LCA estimates from literature [48], even at scales below 2000 MTPD.

If excluding co-product credits (Table 7), renewable diesel produced from CFP has slightly higher GHG emissions (32 g CO_2e MJ^{-1}) compared to that produced from fast pyrolysis (13 g CO_2e/MJ) with catalytic upgrading due to its lower yield (116 versus 196 L/dry metric ton) and thus incrementally greater GHG emission contributions from feedstock collection and transport, but also due to differences in input utilities, hydrogen, and catalyst regeneration. The catalytic upgrading process considered a case in which hydrogen for upgrading the bio-oil is produced from the biochar co-product and non-condensable gases, which requires greater electricity input compared to the catalytic pyrolysis process but no additional hydrogen. On the other hand, catalytic pyrolysis requires purchase of hydrogen, which we assume is produced from catalytic cracking of naptha, assuming upgrading occurs at a petroleum refinery; however, it may also be sourced from steam reforming of natural gas, which has a GHG intensity of 14 g CO_2e/kg compared to ~3 g CO_2e/kg from naptha catalytic cracking, according to European data from the GaBi 9 LCA database and software [50,51] for production in Germany and the Netherlands. This could raise the life cycle GHG emissions for CFP by 3 g CO_2e/MJ (Fig. 5) as well as its
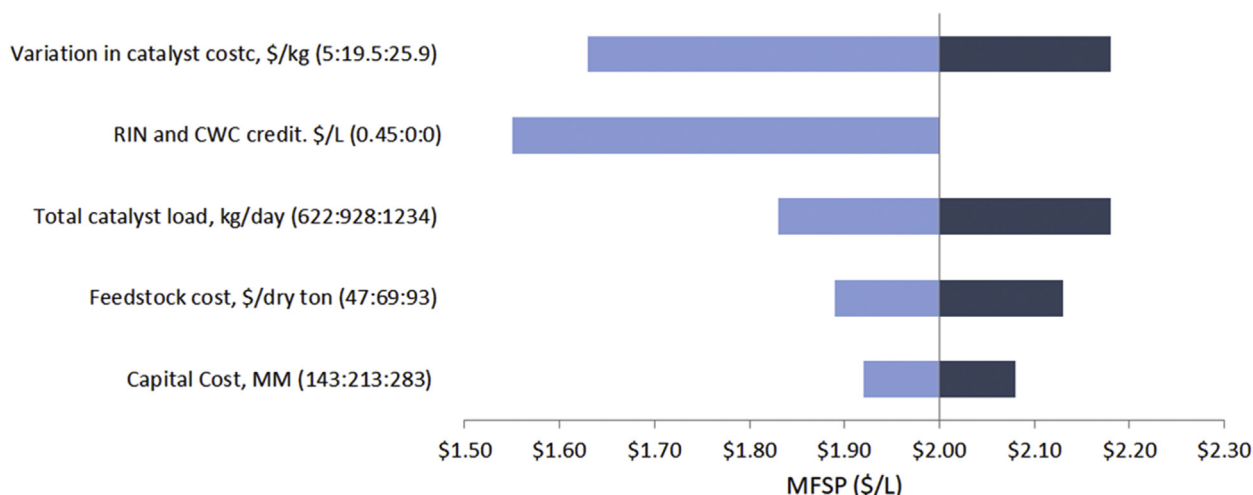

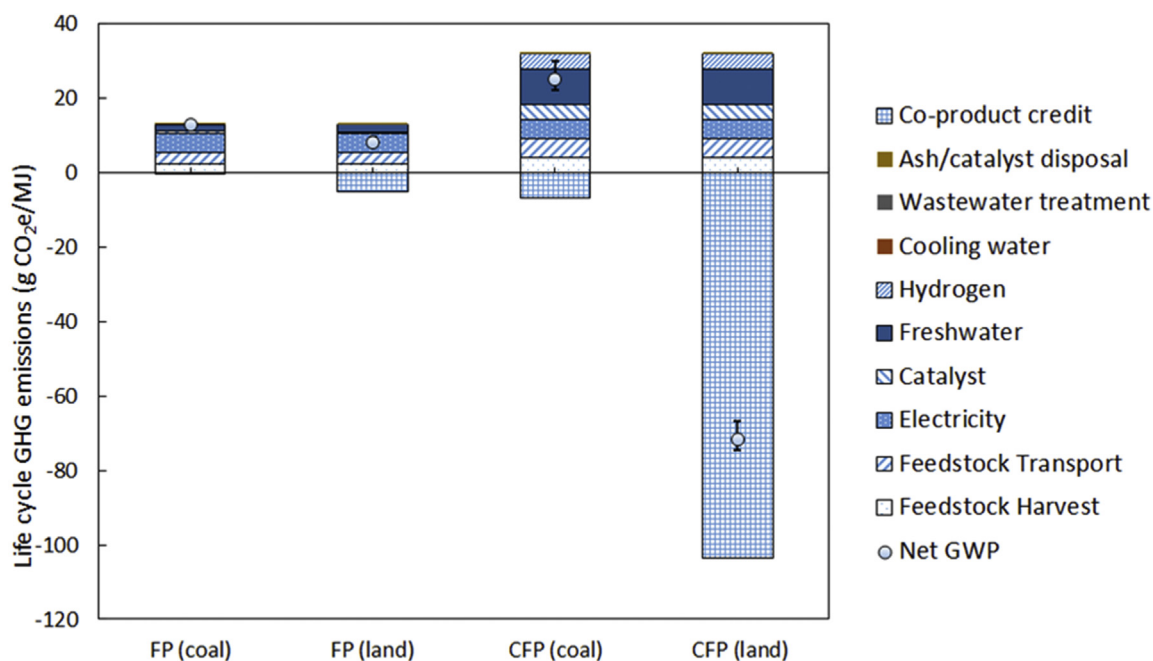**Fig. 3.** Economic Sensitivities for the CFP process on minimum fuel selling price (MFSP).

Fig. 4. Life cycle greenhouse gas emissions for four fast pyrolysis scenarios that include catalysts in upgrading and/or fast pyrolysis.

Table 7
Select TEA metrics and GHG emissions without credits for FP and CFP with upgrading[a].

	CFP with hydrocracking	FP with Catalytic upgrading
Renewable Diesel Yield (L/dry metric ton)	116	196
Biochar Co-product (kg/dry metric ton)	195	16
Biorefinery scale (MTPD)	2000	2000
Minimum fuel selling price ($/L)	2.00	1.68
Feedstock (g CO_{2e} MJ^{-1}):		
Feedstock Harvest	4.3	2.5
Feedstock Transport	5.1	3.0
Biofuel Conversion (g CO_{2e} MJ^{-1}):		
Electricity	5.1	5.1
Catalyst (total):	4.1	0.5
Ni/ZSM-5	0.7	0.09
Co/Mo	N/A	0.2
Ru/C	N/A	0.2
Zeolite	3.4	N/A
Freshwater	9.4	1.9
Hydrogen	4.0	0.0
Cooling water	0.0	<1
Wastewater treatment	0.1	0.1
Ash and spent catalyst disposal	0.2	0.1
Net GHG emissions *without credit* (g CO_{2e} MJ^{-1})	**32**	**13**

[a] N/A, not applicable.

marginal cost.

Daily catalyst regeneration is a significant process input, contributing sizably to operating costs (Table 5, Fig. 3), and can also contribute to variation in life cycle GHG emissions. For CFP, which has a higher GHG emissions contribution due to the input of zeolite catalyst used in the CFP unit, zeolite loading and GHG intensity of the catalyst can raise renewable diesel life cycle GHG emissions by 2–3 g CO_2e/MJ (Fig. 5a). Catalysts also contribute to 13% of GHG emissions for the CFP process, whereas it contributes ~4% for FP, when co-products are not considered. For the systems studied herein, the FP with catalytic upgrading process requires three catalysts, Ni/ZSM-5, Co/Mo, and Ru/C, whereas catalytic pyrolysis assumes use of only zeolite for CFP and Ni/ZSM-5 for hydrocracking. The sensitivity of catalyst loading and GHG intensity for the FP

system (Fig. 5b) shows a very small increase in life cycle GHG emissions from the Ru/C catalyst, which is comparable to prior study by Snowden-Swan et al. [29]. Although the contribution of the catalyst lifetime and loading is significant and contributes substantially to operating costs, it is an overall lower fraction of the life cycle GHG emissions compared to the fraction of chemical and enzyme loadings needed for bioconversion systems [52,53], which can be as high as 30%–40% of the biorefinery GHG emissions budget when co-products are excluded. Finally, low fuel (product) yield and high biochar (co-product) quantity for CFP with hydrocracking either results in relatively higher GHG emissions if the biochar co-product is co-fired with coal compared to a large negative result if land amended. However, product yield along with meeting GHG emissions reduction targets suggest that FP could be more
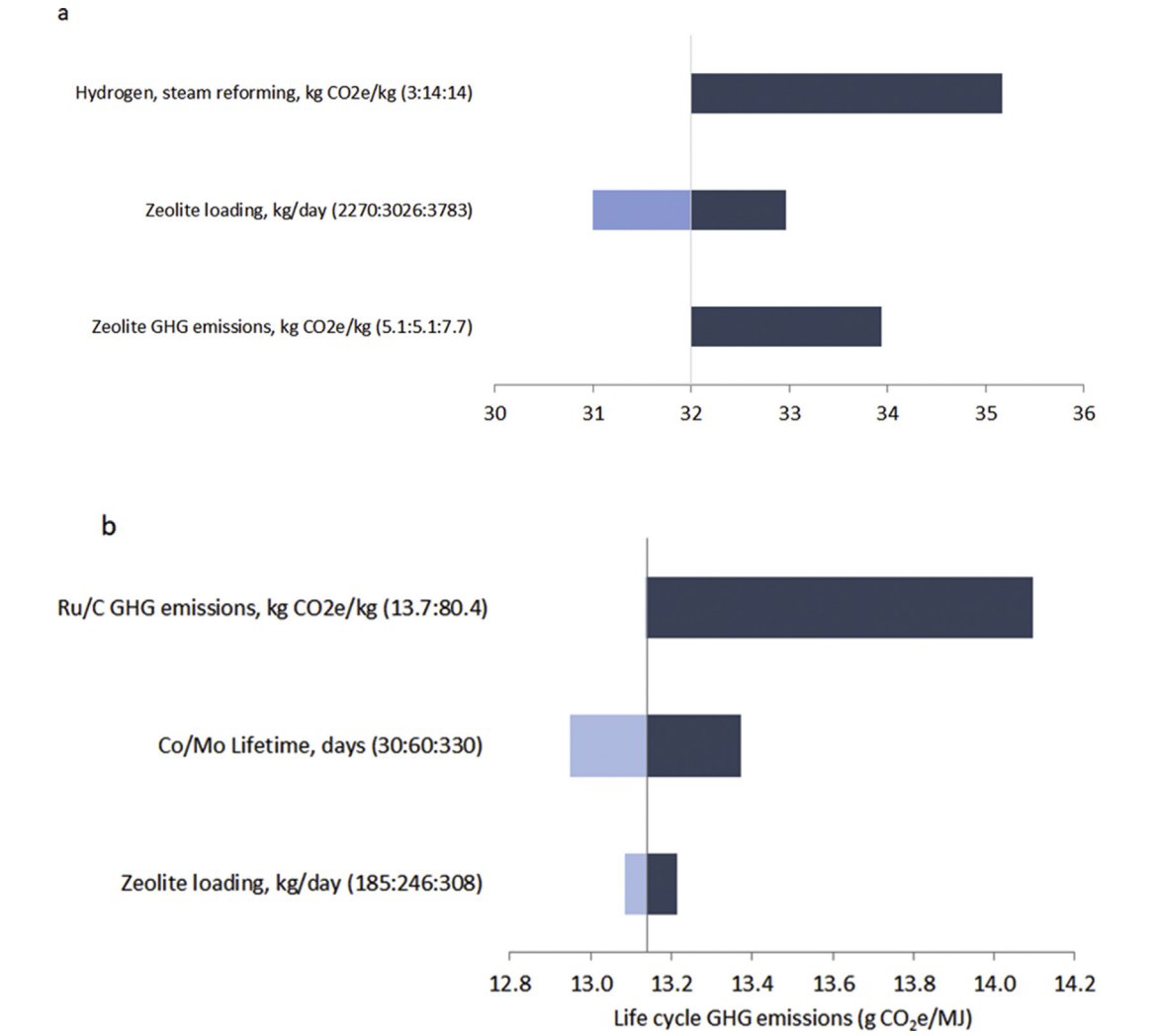
a

b

Fig. 5. Sensitivity of catalyst GHG emissions intensity and loading on life cycle GHG emissions of a) CFP and b) FP renewable diesel pathways.
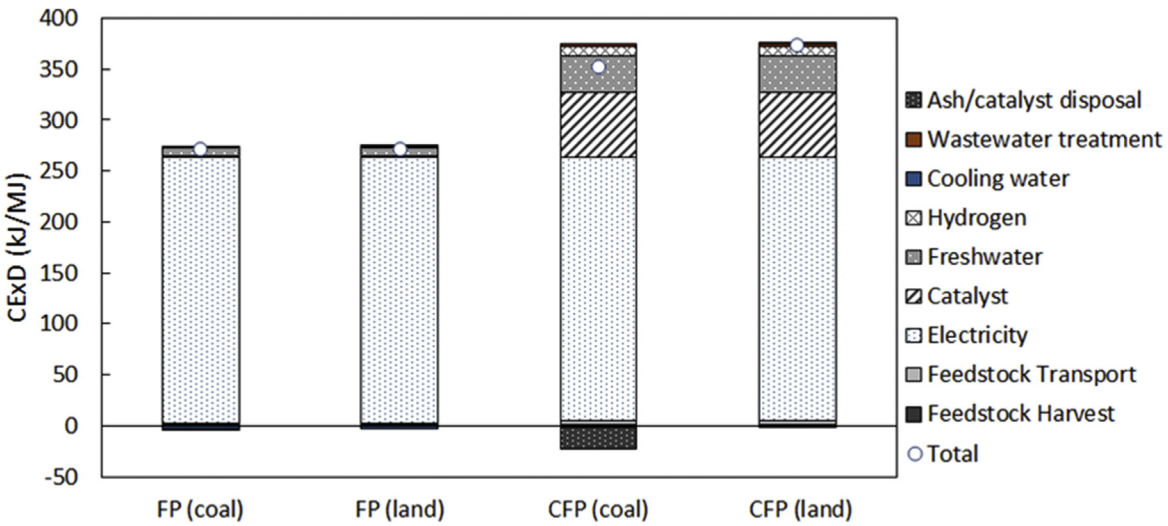

Fig. 6. Cumulative exergy demand for alternative pyrolysis bio-oil upgrading approaches.

favorable than CFP as a commercial process. Moreover, the large biochar yield could be used for producing other value-added products, including hydrogen as with FP, but this would raise capital costs significantly.

3.2.2. Cumulative exergy demand (CExD)

Fig. 6 shows the life cycle effects of cumulative exergy on each MJ of renewable diesel produced. Electricity input is a significant source of exergy for all renewable diesel pathways. In contrast to GHG emissions, CExD results show a higher exergy level for the CFP compared to FP renewable diesel owing to high input of replacement catalyst and water resources, which also suggests that these inputs are energy intensive relative to all other inputs. Only if the co-produced biochar is substituted for coal in power plants is there a credit that reduces CExD, which highlights the observation that the metric for maximum work (and resource efficiency) has less bearing on climate change mitigation aspects.

4. Conclusion

Techno-economic analysis models using experimental data from two pathways for producing commercial-scale renewable diesel from the upgrading of catalytic fast pyrolysis and fast pyrolysis bio-oils are used to generate material balance and energy input data for evaluating economic and environmental performance. While both pathways show potential for a dramatic reduction in GHG emissions relative to low S diesel, meeting advanced RFS2 policy goals in the U.S., tradeoffs among product yield and daily catalyst input and hydrogen demand render both pathways costly, requiring further technological development to improve process economics. Although catalyst contribution to life cycle GHG emissions is not minor, it is small compared to the life cycle contributions of N_2O for growing biomass if coming from agricultural feedstocks and from chemical and enzyme loadings if biochemical conversion processes are employed. Co-product credits can offset a significant fraction of the biorefinery GHG emissions. Even in their absence, catalyst contribution does not prevent pyrolysis-based processes from meeting renewable energy policies. The FP process aims to overcome both the high cost and high GHG emissions associated with purchased hydrogen from fossil energy resources by producing it renewably onsite, whereas the CFP process requires overall greater input of catalyst but saves on capital cost for hydrotreating steps and hydrogen input, sourcing the latter from fossil energy resources to keep both capital and operating costs low. While both pathways meet advanced fuel status within the RFS2, the credits of approximately $0.45 L^{-1} are not high enough to overcome our estimated MFSP to be competitive with low S diesel.

Continued research to improve catalyst lifetime can improve economics and further reduce GHG emissions for renewable diesel from upgraded fast pyrolysis bio-oils. Research by Mullen and Boateng [54] suggests that designing for mid-level deoxygenation to oxygen contents of 25 wt% in a catalytic fast pyrolysis process followed by mild hydrotreating steps may improve carbon yield and subsequent hydrogenation response during hydrotreating, yielding some aromatic ring saturation and higher H/C ratio. Such changes that optimize product yield will improve both economic and environmental performance.

Author contributions

S.S., C.A.M and A.A.B conceived the work. S.S. completed the LCA, policy analysis and wrote the manuscript. V.L. and I.M. completed the Aspen Plus and techno-economic analysis calculations with guidance from M.C.W. and C.A.M. N.A.M and A.A.B.

developed the ideas for exergetic LCA applied to fast pyrolysis upgrading systems. All authors contributed to reviewing and editing the manuscript.

CRediT authorship contribution statement

S. Spatari: Writing - original draft, Formal analysis, Writing - review & editing, conceived the work, completed the LCA, policy analysis and wrote the manuscript. All authors contributed to reviewing and editing the manuscript. **V. Larnaudie:** Formal analysis, Writing - review & editing, completed the Aspen Plus and techno-economic analysis calculations with guidance. All authors contributed to reviewing and editing the manuscript. **I. Mannoh:** Formal analysis, Writing - review & editing, completed the Aspen Plus and techno-economic analysis calculations with guidance. All authors contributed to reviewing and editing the manuscript. **M.C. Wheeler:** Formal analysis, Writing - review & editing, completed the Aspen Plus and techno-economic analysis calculations with guidance. eveloped the ideas for exergetic LCA applied to fast pyrolysis upgrading systems., All authors contributed to reviewing and editing the manuscript. **N.A. Macken:** Formal analysis, Writing - review & editing, completed the Aspen Plus and techno-economic analysis calculations with guidance. developed the ideas for exergetic LCA applied to fast pyrolysis upgrading systems. All authors contributed to reviewing and editing the manuscript.. **C.A. Mullen:** Formal analysis, Writing - review & editing, conceived the work, completed the Aspen Plus and techno-economic analysis calculations with guidance from, eveloped the ideas for exergetic LCA applied to fast pyrolysis upgrading systems, All authors contributed to reviewing and editing the manuscript. **A.A. Boateng:** Writing - review & editing, conceived the work. developed the ideas for exergetic LCA applied to fast pyrolysis upgrading systems. All authors contributed to reviewing and editing the manuscript.

Declaration of competing interest

The authors declare that they have no known competing financial interests or personal relationships that could have appeared to influence the work reported in this paper.

Acknowledgments

Appendix A. Supplementary data

Supplementary data to this article can be found online at https://doi.org/10.1016/j.renene.2020.08.042.

References

[1] C. Fertitta-Roberts, S. Spatari, D.A. Grantz, G.D. Jenerette, Trade-offs across productivity, GHG intensity, and pollutant loads from second-generation sorghum bioenergy, GCB Bioenergy 9 (12) (2017) 1764–1779, https://doi.org/10.1111/gcbb.12471.

[2] F. Creutzig, N.H. Ravindranath, G. Berndes, S. Bolwig, R. Bright, F. Cherubini, H. Chum, E. Corbera, M. Delucchi, A. Faaij, J. Fargione, H. Haberl, G. Heath, O. Lucon, R. Plevin, A. Popp, C. Robledo-Abad, S. Rose, P. Smith, A. Stromman, S. Suh, O. Masera, Bioenergy and climate change mitigation: an assessment, GCB Bioenergy 7 (5) (2015) 916–944, https://doi.org/10.1111/gcbb.12205.

[3] US EPA, Renewable Fuel Standard Program (RFS2) Regulatory Impact Analysis, United States Environmental Protection Agency, Washington, D.C., 2010. Washington, DC, Washington, DC.

[4] Department for Transport, Consultation on the Draft Renewable Transport Fuel Obligations Order 2007, UK Department for Transport, London, 2006, p. 104.

[5] European Union, in: E. Union (Ed.), Directive 2009/28/EC of the European Parliament and of the Council of 23 April 2009 on the Promotion of the Use of

Energy from Renewable Sources and Amending and Subsequently Repealing Directives 2001/77/EC and 2003/30/EC (PDF), 2009. Brussels, Belgium.

[6] S. Yeh, J. Witcover, G.E. Lade, D. Sperling, A review of low carbon fuel policies: principles, program status and future directions, Energy Pol. 97 (2016) 220—234.

[7] V. Larnaudie, M. Bule, K.-Y. San, P.V. Vadlani, J. Mosby, S. Elangovan, M. Karanjikar, S. Spatari, Life cycle environmental and cost evaluation of renewable diesel production, Fuel 279 (2020) 118429, https://doi.org/10.1016/j.fuel.2020.118429.

[8] S. van Dyk, J Su, J.D. Mcmillan, J. Saddler, Potential synergies of drop-in biofuel production with further co-processing at oil refineries, Biofuels, Bioproducts and Biorefining 13 (3) (2019) 760—775.

[9] S. Geleynse, K. Brandt, M. Garcia-Perez, M. Wolcott, X. Zhang, The alcohol-to-jet conversion pathway for drop-in biofuels: techno-economic evaluation, ChemSusChem 11 (21) (2018) 3728—3741.

[10] N.R. Baral, O. Kavvada, D. Mendez-Perez, A. Mukhopadhyay, T.S. Lee, B.A. Simmons, C.D. Scown, Techno-economic analysis and life-cycle greenhouse gas mitigation cost of five routes to bio-jet fuel blendstocks, Energy Environ. Sci. 12 (3) (2019) 807—824.

[11] J. Han, L. Tao, M. Wang, Well-to-wake analysis of ethanol-to-jet and sugar-to-jet pathways, Biotechnol. Biofuels 10 (1) (2017) 21.

[12] N.R. Baral, E.R. Sundstrom, L. Das, J. Gladden, A. Eudes, J.C. Mortimer, S.W. Singer, A. Mukhopadhyay, C.D. Scown, Approaches for more efficient biological conversion of lignocellulosic feedstocks to biofuels and bioproducts, ACS Sustain. Chem. Eng. 7 (10) (2019) 9062—9079.

[13] B. Riazi, M. Karanjikar, S. Spatari, Renewable rubber and jet fuel from biomass: evaluation of greenhouse gas emissions and land use trade-offs in energy and material markets, ACS Sustain. Chem. Eng. 6 (11) (2018) 14414—14422, https://doi.org/10.1021/acssuschemeng.8b03098.

[14] K.L. Brandt, R.J. Wooley, S.C. Geleynse, J. Gao, J. Zhu, R.P. Cavalieri, M.P. Wolcott, Impact of co-product selection on techno-economic analyses of alternative jet fuel produced with forest harvest residuals, Biofuels, Bioproducts and Biorefining 14 (4) (2020) 764—775.

[15] A. O'Connell, M. Kousoulidou, L. Lonza, W. Weindorf, Considerations on GHG emissions and energy balances of promising aviation biofuel pathways, Renew. Sustain. Energy Rev. 101 (2019) 504—515.

[16] M. Balakrishnan, E.R. Sacia, S. Sreekumar, G. Gunbas, A.A. Gokhale, C.D. Scown, F.D. Toste, A.T. Bell, Novel pathways for fuels and lubricants from biomass optimized using life-cycle greenhouse gas assessment, Proc. Natl. Acad. Sci. Unit. States Am. 112 (25) (2015) 7645—7649.

[17] Y.E. Sorunmu, P. Billen, Y. Elkasabi, C.A. Mullen, N.A. Macken, A.A. Boateng, S. Spatari, Fuels and chemicals from equine-waste-derived tail gas reactive pyrolysis oil: technoeconomic analysis, environmental and exergetic life cycle assessment, ACS Sustain. Chem. Eng. 5 (10) (2017) 8804—8814, https://doi.org/10.1021/acssuschemeng.7b01609.

[18] Y. Zhang, G. Hu, R.C. Brown, Life cycle assessment of the production of hydrogen and transportation fuels from corn stover via fast pyrolysis, Environ. Res. Lett. 8 (2) (2013), 025001.

[19] G.G. Zaimes, A.W. Beck, R.R. Janupala, D.E. Resasco, S.P. Crossley, L.L. Lobban, V. Khanna, Multistage torrefaction and in situ catalytic upgrading to hydrocarbon biofuels: analysis of life cycle energy use and greenhouse gas emissions, Energy Environ. Sci. 10 (5) (2017) 1034—1050.

[20] D.D. Hsu, Life cycle assessment of gasoline and diesel produced via fast pyrolysis and hydroprocessing, Biomass Bioenergy 45 (2012) 41—47, 0.

[21] O. Winjobi, W. Zhou, D. Kulas, J. Nowicki, D.R. Shonnard, Production of hydrocarbon fuel using two-step torrefaction and fast pyrolysis of pine. Part 2: life-cycle carbon footprint, ACS Sustain. Chem. Eng. 5 (6) (2017) 4541—4551.

[22] L. Heng, H. Zhang, J. Xiao, R. Xiao, Life cycle assessment of polyol fuel from corn stover via fast pyrolysis and upgrading, ACS Sustain. Chem. Eng. 6 (2) (2018) 2733—2740.

[23] Y. Sorunmu, P. Billen, S.E. Elangovan, D. Santosa, S. Spatari, Life-cycle assessment of alternative pyrolysis-based transport fuels: implications of upgrading technology, scale, and hydrogen requirement, ACS Sustain. Chem. Eng. 6 (8) (2018) 10001—10010, https://doi.org/10.1021/acssuschemeng.8b01266.

[24] W. Liu, J. Wang, T.L. Richard, D.S. Hartley, S. Spatari, T.A. Volk, Economic and life cycle assessments of biomass utilization for bioenergy products, Biofuels, Bioproducts and Biorefining 11 (4) (2017) 633—647, https://doi.org/10.1002/bbb.1770.

[25] Z. Wang, J.B. Dunn, J. Han, M.Q. Wang, Effects of co-produced biochar on life cycle greenhouse gas emissions of pyrolysis-derived renewable fuels, Biofuels, Bioproducts and Biorefining 8 (2) (2014) 189—204.

[26] G. Pourhashem, S.Y. Hung, K.B. Medlock, C.A. Masiello, Policy support for biochar: review and recommendations, GCB Bioenergy 11 (2) (2019) 364—380, https://doi.org/10.1111/gcbb.12582.

[27] E. Furimsky, Catalytic hydrodeoxygenation, Appl. Catal. Gen. 199 (2) (2000) 147—190.

[28] P.T. Benavides, D.C. Cronauer, F. Adom, Z. Wang, J.B. Dunn, The influence of catalysts on biofuel life cycle analysis (LCA), Sustainable Materials and Technologies 11 (2017) 53—59.

[29] L.J. Snowden-Swan, K.A. Spies, G.J. Lee, Y. Zhu, Life cycle greenhouse gas emissions analysis of catalysts for hydrotreating of fast pyrolysis bio-oil, Biomass Bioenergy 86 (2016) 136—145.

[30] ISO, ISO 14040: Environmental Management — Life Cycle Assessment — Principles and Framework, International Organization for Standardization Geneva, 2006.

[31] ISO, ISO 14044: Environmental Management — Life Cycle Assessment — Requirements and Guidelines, International Organization for Standardization, Geneva, 2006.

[32] C.A. Mullen, A.A. Boateng, D.J. Mihalcik, N.M. Goldberg, Catalytic fast pyrolysis of white oak wood in a bubbling fluidized bed, Energy Fuel. 25 (11) (2011) 5444—5451.

[33] J.L. Carrasco, S. Gunukula, A.A. Boateng, C.A. Mullen, W.J. DeSisto, M.C. Wheeler, Pyrolysis of forest residues: an approach to techno-economics for bio-fuel production, Fuel 193 (2017) 477—484.

[34] G. Pourhashem, S. Spatari, A.A. Boateng, A.J. McAloon, C.A. Mullen, Life cycle environmental and economic tradeoffs of using fast pyrolysis products for power generation, Energy Fuel. 27 (5) (2013) 2578—2587, https://doi.org/10.1021/ef3016206.

[35] M.E. Bösch, S. Hellweg, M.A.J. Huijbregts, R. Frischknecht, Applying cumulative exergy demand (CExD) indicators to the ecoinvent database, Int. J. Life Cycle Assess. 12 (3) (2006) 181.

[36] J. Keedy, E. Prymak, N. Macken, G. Pourhashem, S. Spatari, C.A. Mullen, A.A. Boateng, Exergy based assessment of the production and conversion of switchgrass, equine waste, and forest residue to bio-oil using fast pyrolysis, Ind. Eng. Chem. Res. 54 (1) (2015) 529—539, https://doi.org/10.1021/ie5035682.

[37] M.E. Hums, R.A. Cairncross, S. Spatari, Life-cycle assessment of biodiesel produced from grease trap waste, Environ. Sci. Technol. 50 (5) (2016) 2718—2726, https://doi.org/10.1021/acs.est.5b02667.

[38] I. Dincer, M. Rosen, Exergy Energy, Environment and Sustainable Development, second ed. ed., Elsevier, 2013.

[39] D. Humbird, R. Davis, L. Tao, C. Kinchin, D. Hsu, A. Aden, P. Schoen, J. Lukas, B. Olthof, M. Worley, D. Sexton, D. Dudgeon, Process Design and Economics for Biochemical Conversion of Lignocellulosic Biomass to Ethanol, National Renewable Energy Laboratory, 2011.

[40] M.S. Booth, B. Mackey, V. Young, It's time to stop pretending burning forest biomass is carbon neutral, GCB Bioenergy 10.1111/gcbb.12716.

[41] E.-D. Schulze, C. Körner, B.E. Law, H. Haberl, S. Luyssaert, Large-scale bioenergy from additional harvest of forest biomass is neither sustainable nor greenhouse gas neutral, GCB Bioenergy 4 (6) (2012) 611—616.

[42] G. Wernet, C. Bauer, B. Steubing, J. Reinhard, E. Moreno-Ruiz, B. Weidema, The ecoinvent database version 3 (part I): overview and methodology, Int. J. Life Cycle Assess. 21 (9) (2016) 1218—1230.

[43] Z. Wang, P.T. Benavides, J.B. Dunn, D.C. Cronauer, Development of GREET Catalyst Module, Argonne National Lab. (ANL), Argonne, IL (United States), 2015, p. 53. Medium: ED; Size.

[44] A. Dutta, A. Sahir, E. Tan, D. Humbird, L.J. Snowden-Swan, P. Meyer, J. Ross, D. Sexton, R. Yap, J.L. Lukas, Process Design and Economics for the Conversion of Lignocellulosic Biomass to Hydrocarbon Fuels. Thermochemical Research Pathways with in Situ and Ex Situ Upgrading of Fast Pyrolysis Vapors, NREL (National Renewable Energy Laboratory (NREL), Golden, CO (United States)), 2015.

[45] S. Dillich, T. Ramsden, M. Melaina, Hydrogen Production Cost Using Low-Cost Natural Gas, DOE Hydrogen and Fuel Cells Program Record, Department of Energy, United States, 2012.

[46] R. Turton, R.C. Bailie, W.B. Whiting, J.A. Schaeiwitz, D. Bhattacharyya, Analysis, Synthesis, and Design of Chemical Processes, third ed., Prentice Hall, Upper Saddle River, New Jersey, 2009.

[47] S.B. Jones, J. Holladay, C. Valkenburg, D. Stevens, C. Walton, C. Kinchin, D. Elliott, S. Czernik, Production of gasoline and diesel from biomass via fast pyrolysis, Hydrotreating and Hydrocracking: A Design Case (2009) 76.

[48] Y. Sorunmu, P. Billen, S. Spatari, A review of thermochemical upgrading of pyrolysis bio-oil: techno-economic analysis, life cycle assessment, and technology readiness, GCB Bioenergy 12 (1) (2020) 4—18, https://doi.org/10.1111/gcbb.12658.

[49] M. Worley, J. Yale, Biomass Gasification Technology Assessment: Consolidated Report, National Renewable Energy Laboratory (NREL), Golden, CO., 2012.

[50] S. Spatari, M. Betz, H. Florin, M. Baitz, M. Faltenbacher, Using GaBi 3 to perform life cycle assessment and life cycle engineering, Int. J. Life Cycle Assess. 6 (2) (2001) 81—84, https://doi.org/10.1007/bf02977842.

[51] Sphera, GaBi 9: the Software System for Life Cycle Assessment, 2020. Stuttgart.

[52] S. Spatari, D.M. Bagley, H.L. MacLean, Life cycle evaluation of emerging lignocellulosic ethanol conversion technologies, Bioresour. Technol. 101 (2) (2010) 654—667, https://doi.org/10.1016/j.biortech.2009.08.067.

[53] H.L. MacLean, S. Spatari, The contribution of enzymes and process chemicals to the life cycle of ethanol, Environ. Res. Lett. 1 (2009), 014001, https://doi.org/10.1088/1748-9326/4/1/014001.

[54] C.A. Mullen, A.A. Boateng, Mild hydrotreating of bio-oils with varying oxygen content produced via catalytic fast pyrolysis, Fuel 245 (2019) 360—367, https://doi.org/10.1016/j.fuel.2019.02.027.